

Collaborative Semantic Aggregation and Calibration for Separated Domain Generalization

Junkun Yuan, *Student Member, IEEE*, Xu Ma, Defang Chen, Kun Kuang, Fei Wu, *Senior Member, IEEE*, and Lanfen Lin, *Member, IEEE*,

Abstract—Domain generalization (DG) aims to learn from multiple known source domains a model that can generalize well to unknown target domains. The existing DG methods usually exploit the fusion of shared multi-source data for capturing domain invariance and training a generalizable model. However, tremendous data is distributed across lots of places nowadays that can not be shared due to strict privacy policies. A dilemma is thus raised between the generalization learning with shared multi-source data and the privacy protection of real-world sensitive data. In this paper, we introduce a separated domain generalization task with separated source datasets that can only be accessed locally for data privacy protection. We propose a novel solution called Collaborative Semantic Aggregation and Calibration (CSAC) to enable this challenging task. To fully absorb multi-source semantic information while avoiding unsafe data fusion, we conduct data-free semantic aggregation by fusing the models trained on the separated domains layer-by-layer. To address the semantic dislocation problem caused by domain shift, we further design cross-layer semantic calibration with an elaborate attention mechanism to align each semantic level and enhance domain invariance. We unify multi-source semantic learning and alignment in a collaborative way by repeating the semantic aggregation and calibration alternately, keeping each dataset localized, and the data privacy is thus carefully protected. Extensive experiments show the significant performance of our method in addressing this challenging task, which is even comparable to the previous DG methods with shared source data.

Index Terms—Separated domain generalization, visual recognition, semantic aggregation and calibration, privacy protection.

I. INTRODUCTION

RECENTLY, deep learning has made revolutionary advances to visual recognition [17], under the i.i.d. assumption that training and test data should be sampled from the same statistical distribution. Since the adopted datasets could be very distinct in many real-world applications, the performance of deep models learned from one training (source) dataset may drop rapidly on another test (target) dataset. To address this *dataset/domain shift* [43] problem, *domain generalization* (DG) [3] is introduced for training a generalizable model to unknown out-of-distribution target domains by learning from multiple semantically relevant source domains.

Manuscript received January 19, 2022.

(Corresponding author: Kun Kuang.)

(Junkun Yuan and Xu Ma contributed equally to this work.)

J. Yuan, X. Ma, D. Chen, K. Kuang, F. Wu, and L. Lin are with the College of Computer Science and Technology, Zhejiang University, Hangzhou 310027, China (e-mail: yuanjk@zju.edu.cn; maxu@zju.edu.cn; defchern@zju.edu.cn; kunkuang@zju.edu.cn; wufei@cs.zju.edu.cn; llf@zju.edu.cn).

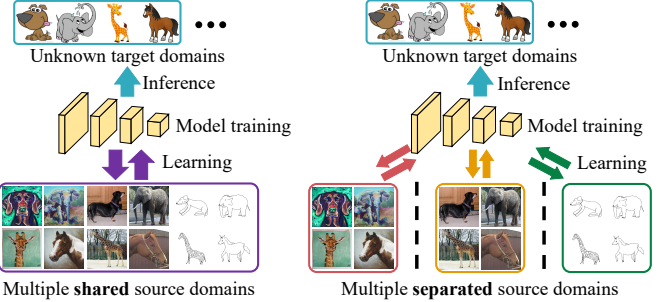


Fig. 1. Comparison of the domain generalization task (left) and the introduced separated domain generalization task (right). The latter realizes privacy protection when training generalizable models in many privacy-sensitive scenarios.

Numerous DG methods [4], [9], [64] have been proposed recently. They popularize a variety of favorable strategies for training generalizable models by (indirectly) exploiting the fusion of “*shared*” multi-source data. For example, some alignment-based methods [24], [27], [64] match source data distributions in latent space for generating domain-invariant feature representations; and some meta-learning based strategies [9], [23], [30] utilize meta-train and meta-test datasets built by sampling from multi-source data for training a stable model to unknown domains. However, these methods may seriously violate data privacy policies, as tremendous data is stored locally in distributed places nowadays which may contain private information, e.g., the patient data from hospitals and the video recording from surveillance cameras. Therefore, a dilemma is encountered: The requirements of learning from shared multi-source data for training a highly generalizable model may hard to be met in many real scenarios due to the privacy issues; While without simultaneous access to the source datasets for obtaining adequate information of multi-source distribution, identifying and learning domain invariance for improving model generalization might be led astray.

In this paper, we introduce *separated domain generalization* (see Fig. 1), where the source datasets are separated and can only be accessed locally. It enables privacy preserving of sensitive data when employing them for improving model generalization, however, is much more challenging as: The separated source datasets are private and may not be directly fused, hence the simultaneous learning of the multi-source semantic information is greatly hindered, making the identification of domain invariance tricky; While the heterogeneous source datasets with distinct data distributions may constitute enormous obstacles for training a generalizable model as the

model is allowed to access only one local dataset each time, while the accessed dataset could contain particularly unusual bias and even bring negative gain for model generalization.

We propose a novel method called Collaborative Semantic Aggregation and Calibration (CSAC) to enable separated domain generalization. We begin by hypothesizing that the deep models extract semantic information from low-level to high-level, and the model parameters in each layer are related to the corresponding semantic level as well as the training data distribution (proof-of-concept experiments are provided to verify it). In light of this, to fully absorb multi-source semantic information while avoiding risky data fusion, a data-free semantic aggregation strategy is devised to fuse the models trained on the separated domains layer-by-layer. Then a semantic dislocation problem has arisen: Due to domain shift, the same level of semantic information from different domains could be distributed across model layers during the aggregation. To this end, we further design cross-layer semantic calibration with an elaborate attention mechanism for precise semantic level alignment and domain-invariance enhancement. We unify the multi-source semantic learning and alignment in a collaborative way by repeating the semantic aggregation and calibration alternately. Each source dataset contributes semantic information locally for boosting model generalization during this process, resulting in a high-quality generalizable model under effective data privacy protection.

Our main contributions are: (1) We introduce a separated domain generalization task to tackle the dilemma between the generalization learning with shared multi-source data and the privacy protection of real-world sensitive data for realizing practical generalizable model training in real scenarios; (2) To enable separated domain generalization, we propose a novel privacy-preserving method called Collaborative Semantic Aggregation and Calibration (CSAC) to unify the multi-source semantic learning and alignment in a collaborative way by repeating data-free semantic aggregation and cross-layer semantic calibration alternately; (3) Extensive experiments on benchmark datasets show significant performance of our method for separated domain generalization, which is even comparable to the previous DG methods with shared data.

II. RELATED WORK

A. Domain Adaptation

To address the widespread domain shift problem, remarkable progress [12], [28], [32], [49], [53], [54], [62], [63], [68] has been made in domain adaptation task. It aims to adapt a model trained on source domains to target domains by exploiting target data/information. One prevailing direction for this task is to employ adversarial learning [5], [32], [50] for reducing domain gap and generating domain-agnostic representations. Meanwhile, some algorithms [7], [28] are put forward to directly minimize domain divergence with distance metric like Maximum Mean Discrepancies (MMD). However, the target data/information is assumed to be available in this task, which greatly limits its implementation in many real-world applications where collecting adequate target data and information might be extremely expensive and laborious.

B. Domain Generalization

Domain generalization (DG) [3], [8], [23], [25], [30], [36], [41], [58], [59], [64] aims to train a stable model to unknown target domains by learning invariant knowledge from multiple source domains. A direct idea for DG is to align multi-source data distributions in latent space for generating invariant semantic representation [24], [25], [27], [29], [36], [41], [42], [64]. For example, Li et al. [29] extract domain-invariant representations of multi-source joint distributions through a conditional invariant adversarial network. Another set of works [2], [9], [21], [23], [30] are based on meta-learning, they employ an episodic training paradigm that trains the model and improves its out-of-distribution generalization ability on meta-train and meta-test datasets, respectively, which are built by the shared multi-source data. For instance, Dou et al. [9] present a model-agnostic meta-learning training paradigm with two complementary losses to consider both global knowledge and local cohesion. Data augmentation [4], [45], [47], [51], [65]–[67] for DG is also popular which trains the model on generated novel domains for improving model generalization. Among them, JiGen [4] is a representative work that utilizes the data with disordered patches to train the model for solving a jigsaw puzzle. Some other works [6], [18], [44] optimize the regularization terms of the data or networks to obtain generalization performance gain. These methods are mostly in thrall to shared multi-source data for identifying domain invariance and boosting model generalization, while concerns about data privacy are thus raised as tremendous private data might be distributed across separated places in many real scenarios. In comparison, we introduce separated domain generalization towards privacy-preserving generalizable model training by accessing and learning each source dataset locally.

C. Federated Learning

As an active research field towards modern privacy protection, federated learning [13], [33], [38], [56], [57] makes local clients jointly train a model with a central server and keeps data decentralized. Take a representative paradigm FedAvg [38] as an example. In each communication round, a subset of the clients is chosen to receive the parameters of a global model from the server and trains it on their local data. The trained models are then transmitted back to the server for updating the global model with data-size based weights. Our investigated separated domain generalization task is closely related to federated learning as the data is decentralized, but the former is much more challenging: FL mainly focuses on guaranteeing model convergence when training on non-i.i.d. data [56], and improving model performance on the “*known*” clients; In contrast, our goal is to capture domain invariance from the separated source domains and train a generalizable model for the “*unknown*” out-of-distribution target domains.

D. Distributed Domain Adaptation and Generalization

Source-free domain adaptation [20], [26] improves performance on the target domain by using a source pre-trained model. Federated learning based domain adaptation

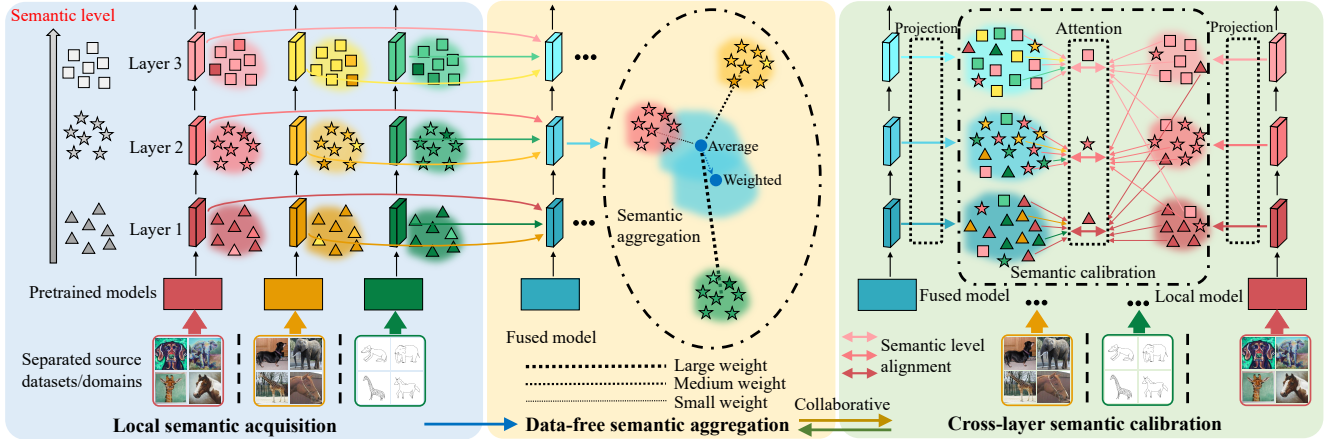


Fig. 2. Overview of the proposed Collaborative Semantic Aggregation and Calibration (CSAC). Left: To extract distribution information of local data, each domain trains a model which extracts semantics from low-level to high-level, i.e., \blacktriangle , \star , and \blacksquare ; Middle: The trained models are fused layer-by-layer with semantic divergence based weights for semantic gathering; Right: Cross-layer feature pairs between the fused model and each local model are matched with attention for semantic level alignment and domain invariance enhancement. After semantic acquisition, the aggregation and calibration work collaboratively.

[40] adapts models from distributed source domains to target domains. However, these methods are limited to the strong assumption of available target data/information, as we discussed previously. FedDG [34] is proposed to learn a generalizable model in federated learning setting with frequency space interpolation for medical image segmentation. However, it builds an amplitude spectrum distribution bank from the source data and shares it to all the clients, which: (1) is time-consuming for building the bank and expensive for data storage; (2) needs high communication costs to transmit the bank to all the clients; (3) shares the amplitude spectrum of the source data to all the clients that may increase the risks of data privacy leakage. In comparison, our proposed method do not have extra time-consuming procedures like building such a distribution bank. More importantly, we do not share any data (or parts of its information) during model training for efficient communication and effective data privacy protection.

III. METHOD

We begin with the problem definition of the introduced separated domain generalization and its challenges for generalizable model training. We then introduce our method CSAC (see Fig. 2) for addressing this challenging task in detail.

A. Separated Domain Generalization

In separated domain generalization, we have source datasets $\{\mathcal{D}^1, \dots, \mathcal{D}^H\}$ from H separated domains. There are N^h samples in each dataset \mathcal{D}^h , i.e., $\mathcal{D}^h = \{(x_i^h, y_i^h)\}_{i=1}^{N^h}$, defined on image and label spaces $\mathcal{X} \times \mathcal{Y}$. The goal is to utilize the separated source datasets for training a generalizable model, which can perform well on unknown target domains. Note that FedDG [34] may consider thousands of heterogeneous clients for model training, while our separated domain generalization task mainly focuses on multiple homogeneous source datasets with the same data spaces but different data distributions.

The challenges of this task are: (1) The source datasets are separated and can only be utilized locally, which greatly

hinders the simultaneous learning of the multi-source semantic information and even leads to invalid domain invariance identification; (2) The heterogeneous source datasets with distinct data distributions constitute enormous obstacles for generalizable model training, as the model can only access one local data each time. That is, if one exploited local dataset contains particularly unusual domain-specific bias, the trained model may even exhibit a negative generalization gain.

The key idea of our method CSAC (Fig. 2) is to fully absorb multi-source information and precisely align semantic levels, which contains three main processes: (1) *Local semantic acquisition* for extracting distribution information of local data; (2) *Data-free semantic aggregation* for semantic information gathering from the trained local models; and (3) *Cross-layer semantic calibration* for semantic level alignment and domain invariance enhancement. After obtaining local distribution information in process (1), the latter two processes are repeated alternately, unifying the multi-source semantic learning and alignment in a collaborative way for generalizable model training. It is worth mentioning that *we only transmit models among the separated domains*, and neither data nor its information is shared, adequately preserving data privacy.

B. Local Semantic Acquisition

Before gathering and aligning the multi-source semantic information, we need to fully absorb the data distribution information of the separated source datasets. To avoid unsafe data fusion, we assign one model on each of the separated domains to impose data distribution learning. Given H separated source datasets, y^h with C categories is the ground-truth label of the image x^h in dataset \mathcal{D}^h , where $h \in \{1, \dots, H\}$. Let $\{G^h\}_{h=1}^H$ be the trained models, each model G^h can be optimized on the local source data \mathcal{D}^h with the following cross-entropy loss:

$$\mathcal{L}_{CE}^h = -\mathbb{E}_{(x^h, y^h) \in \mathcal{D}^h} \left[\sum_{c=1}^C \mathbb{1}(y^h = c) \log G^{h,c}(x^h) \right], \quad (1)$$

where $G^{h,c}$ is the c -th dimension of the output of model G^h . $\mathbb{1}(\cdot)$ is an indicator function values 1 for the correct condi-

tion and 0 for the rest. To facilitate the following semantic aggregation and calibration processes, we further introduce label smoothing [31], [39] to encourage data representations to group in tight evenly clusters, preventing the trained models from being over-confident. The updated learning loss is

$$\mathcal{L}_{LS}^h = -\mathbb{E}_{(x^h, y^h) \in \mathcal{D}^h} \left[\sum_{c=1}^C p^{h,c} \log G^{h,c}(x^h) \right], \quad (2)$$

where $p^{h,c} = (1 - \alpha) \mathbb{1}(y^h = c) + \alpha/C$ is the smoothed label. α is a smoothing hyper-parameter empirically set to 0.1 [39].

C. Data-Free Semantic Aggregation

After acquiring distribution information of local data, we devise data-free semantic aggregation with the trained models $\{G^h\}_{h=1}^H$. Inspired by recent researches [52], [61] on the interpretability of deep neural networks, we hypothesize that the deep models extract semantic information from low-level to high-level, and the model parameters in each layer are related to the corresponding semantic level as well as the training data distribution (proof-of-concept experiments are shown in Experiments section). As each model G^h trained on the local data \mathcal{D}^h , it extracts hierarchical semantics from data distribution of \mathcal{D}^h . Let G_l^h be the l -th layer of G^h , we have an average model parameter distribution in the l -th layer

$$G_l^{AVG} = \frac{1}{H} \sum_{h=1}^H G_l^h. \quad (3)$$

We then find that if a source data have a distribution far from the others, the corresponding model would be considered less as it is also far from the average distribution G_l^{AVG} . To fairly absorb the information of the source datasets for precise semantic calibration, we assign weight to each model based on its semantic divergence to the average distribution G_l^{AVG} :

$$M_l = \sum_{h=1}^H \frac{\text{dist}(G_l^h, G_l^{AVG})}{\sum_{h=1}^H \text{dist}(G_l^h, G_l^{AVG})} G_l^h, \quad (4)$$

where M_l is the l -th layer of the fused model M , and $\text{dist}(\cdot, \cdot)$ is distance metric and empirically used as L_2 distance. Models with distinct parameters, or training data distributions, will be paid more attention to by being given a large weight. As the trained models are fused layer-by-layer, different levels of semantics from the separated source domains are aggregated for domain invariance learning in the semantic calibration.

D. Cross-Layer Semantic Calibration

Due to the different data distributions of the source datasets, i.e., domain shift, the same level of semantic information from different domains could be distributed across the layers of the fused model M during the aggregation process, which we call the *semantic dislocation* problem. To calibrate each level of semantic information for improving model generalization, we align each cross-layer semantic feature pair between the fused model M and a local model L^h (trained on each local source domain like G^h). Take Fig. 2 (right) as an example. The second layer of the fused model mainly contains the second level

of semantic information from different domains, i.e., \star in different colors. We match it with each layer of a local model to align the second semantic level, i.e., match \star in different layers of the local model, where each cross-layer pair is weighted by their semantic similarities. Since the hierarchical semantic features may have different representation size, we first project them to the same size (we use the size of the semantic features in the last adopted layer in the experiments):

$$\begin{aligned} M_l(x^h)' &= \text{Proj}(M_l(x^h)), \\ L_m^h(x^h)' &= \text{Proj}(L_m^h(x^h)), \end{aligned} \quad (5)$$

where $\text{Proj}(\cdot)$ is the projection function with one convolution layer (see experiments for details). We then align each cross-layer semantic feature pair (l, m) after projection by

$$\mathcal{L}_{AL}^h = \sum_{l \in \mathcal{R}} \sum_{m \in \mathcal{R}} \alpha_{l,m} D(M_l(x^h)', L_m^h(x^h)'), \quad (6)$$

where $D(\cdot, \cdot)$ is used to measure the distribution discrepancy, which is minimized to perform semantic feature alignment. We adopt Maximum Mean Discrepancies (MMD) [16] for it by following [35], [46]. The set of layers \mathcal{R} for alignment is given in experiments. A dynamic weight $\alpha_{l,m}$ for the layer pair (l, m) is learned by attention introduced in the following.

Attention mechanism. To encourage the cross-layer pairs with greater semantic similarity to be matched for precise semantic level alignment and domain invariance enhancement, meanwhile, weakening the pairs with less similarity for avoiding further semantic dislocation, we then introduce a semantic similarity based attention mechanism for the dynamic weight $\alpha_{l,m}$. Attention [1] is a widely adopted technique [10], [48], [60] for deciding which parts of the input features should be paid more attention to. Here, we consider the semantic inter-dependencies in both *position* and *channel* dimensions. Let c , g , and w be the channel, height, and width of the semantic features after projection, respectively. We first reshape $M_l(x)' \in \mathcal{R}^{c \times g \times w}$ and $L_m^h(x)' \in \mathcal{R}^{c \times g \times w}$ to $A_l \in \mathcal{R}^{c \times d}$ and $B_m \in \mathcal{R}^{c \times d}$, respectively, where $d = g \times w$ is the number of pixels in an image. Then, we have a position-wise weight

$$\alpha_{l,m}^p = \frac{\exp(\text{avg}(A_l^\top B_m))}{\sum_{m \in \mathcal{R}} \exp(\text{avg}(A_l^\top B_m))}, \quad (7)$$

where $A_l^\top B_m$ is the position-wise attention map, measuring the response of A_l to B_m , i.e., the l -th layer of the fused model M_l to the m -th layer of the local model L_m^h . The operator $\text{Avg}(\cdot)$ averages the attention map to a real number, and the weight $\alpha_{l,m}^p$ is the normalization of the average position-wise semantic similarity. Similarly, we then have

$$\alpha_{l,m}^c = \frac{\exp(\text{avg}(A_l B_m^\top))}{\sum_{m \in \mathcal{R}} \exp(\text{avg}(A_l B_m^\top))}. \quad (8)$$

$\alpha_{l,m}^c$ measures the channel-wise semantic similarities. We average them to get the final weight for cross-layer pair (l, m) :

$$\alpha_{l,m} = \frac{1}{2} \left(\alpha_{l,m}^p + \alpha_{l,m}^c \right). \quad (9)$$

$\alpha_{l,m}$ characterizes the inter-dependencies between the fused model G_l and each local model L_m^h in both position and

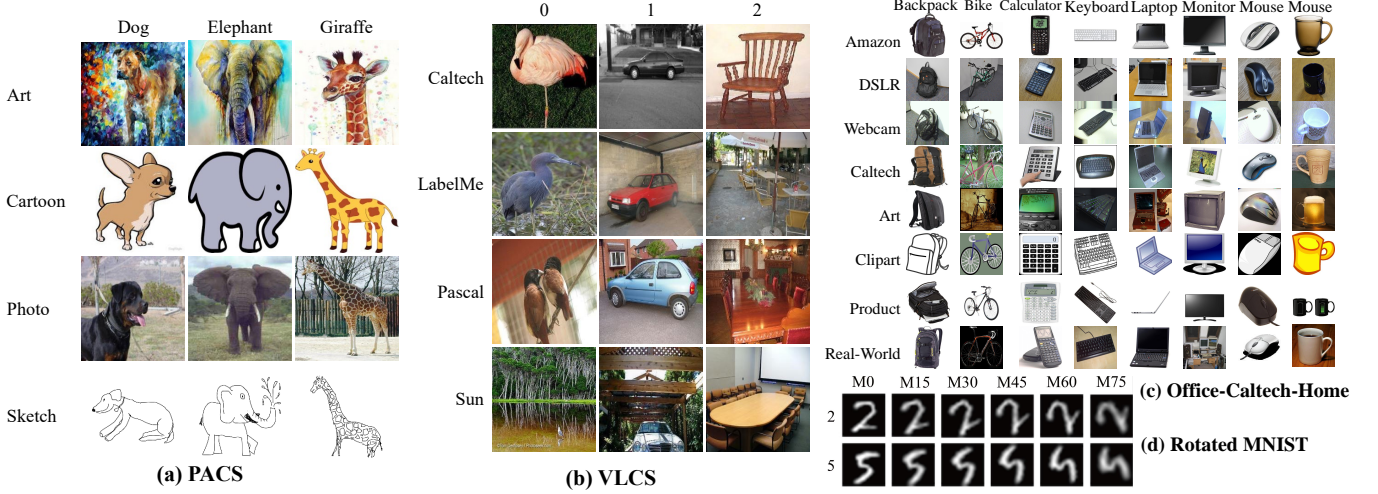


Fig. 3. Some example images of the adopted datasets for experiments, i.e., PACS (a), VLCS (b), Office-Caltech-Home (c), and Rotated MNIST (d).

channel dimensions, weighting cross-layer pairs for calibrating semantic levels and boosting model generalization.

Since the semantic information from each domain is aggregated with others, the fused model may suffer from the *catastrophic forgetting* problem [15], [37], i.e., knowledge from one domain in the model is gradually forgotten when incrementally updating models with knowledge from other domains. We thus employ an auxiliary retraining loss \mathcal{L}_{AR}^h for the model M on each source dataset \mathcal{D}^h , that is,

$$\mathcal{L}_{AR}^h = -\mathbb{E}_{(x^h, y^h) \in \mathcal{D}^h} \left[\sum_{c=1}^C \mathbb{1}(y^h = c) \log M^c(x^h) \right], \quad (10)$$

where M^c is the c -th dimension of the output of the model M . Then we have the calibration loss on each source data \mathcal{D}^h :

$$\mathcal{L}_{CB}^h = \lambda \mathcal{L}_{AL}^h + \mathcal{L}_{AR}^h, \quad (11)$$

where λ is a hyper-parameter for semantic calibration.

E. Model Optimization

We first perform local semantic acquisition by training the local models $\{G^h\}_{h=1}^H$ through Equation (2) for data distribution learning. The trained models are employed to calculate the fused model M for semantic aggregation through Equation (4). We then copy and transmit M to each domain for semantic calibration with Equation (11), and fuse the calibrated models again. We repeat the semantic aggregation and calibration alternately to gather semantic information from separated source domains and calibrate them to enhance domain-invariant semantics, resulting in a highly generalizable model \hat{M} for inference on unknown target domains.

Remark. In practice, we assign the parameters of the fused model M to each trained model G^h for simultaneous semantic calibration on each domain h , and fuse them again.

IV. EXPERIMENTS

A. Setup

In this section, we empirically evaluate the proposed CSAC method for the separated domain generalization task on multi-

ple datasets, and give in-depth ablation studies and discussions. Our code is released as: <https://github.com/junkunyuan/CSAC>.

Benchmark datasets. We first adopt two popular datasets. One is **PACS** [22] that covers 7 categories within 4 domain, i.e., *Art*, *Cartoon*, *Sketch*, *Photo*. Another is **VLCS** [11] that contains 5 classes from 4 domains, i.e., *Pascal*, *LabelMe*, *Caltech*, *Sun*. A simulated digit dataset **Rotated MNIST** [11] is then employed. It has 6 domains, i.e., *M0*, *M15*, *M30*, *M45*, *M60*, *M75*. We use 100 images per class for Rotated MNIST dataset by following [11], [64]. We process the data by following the previous works [18], [64]. To obtain more domains, we construct a new dataset **Office-Caltech-Home** by choosing the common classes from Office-Caltech [14] and Office-Home [46] datasets, and merge them to get 7 domains (DSLR is discarded due to few images), i.e., *Amazon* (*Am*), *Webcam* (*We*), *Caltech* (*Ca*), *Art* (*Ar*), *Clipart* (*Cl*), *Product* (*Pr*), and *Real-World* (*Rw*). Example images of these adopted datasets are given in Fig. 3. We conduct leave-one-domain-out experiments by choosing one domain to hold out as the target domain while the others are used as the source domains.

Baseline methods. We compare our method CSAC against the representative federated learning method *FedAvg* [38] and the federated learning based generalizable model learning method *FedDG* [34] in the separated domain generalization task. We also show the performance of the state-of-the-art DG methods (see Table I and II) introduced in the related work for the domain generalization task with shared source data. We implement baseline of DeepAll by fusing all the source data and directly using it as the source data to train the model.

Implementation details. Following [11], [64], we use standard MNIST CNN architecture with two convolution layers and two fully-connected layers for Rotated MNIST dataset. We use the pretrained ResNet-18 network [17] for PACS, VLCS, and Office-Caltech-Home datasets and also use the AlexNet network [19] for VLCS, following [4], [9], [18]. We extract the convolution layers of the last three blocks of ResNet-18, or the last three convolution layers of AlexNet, or the last two convolution layers of MNIST CNN, as the layer set for semantic calibration. We implement the methods

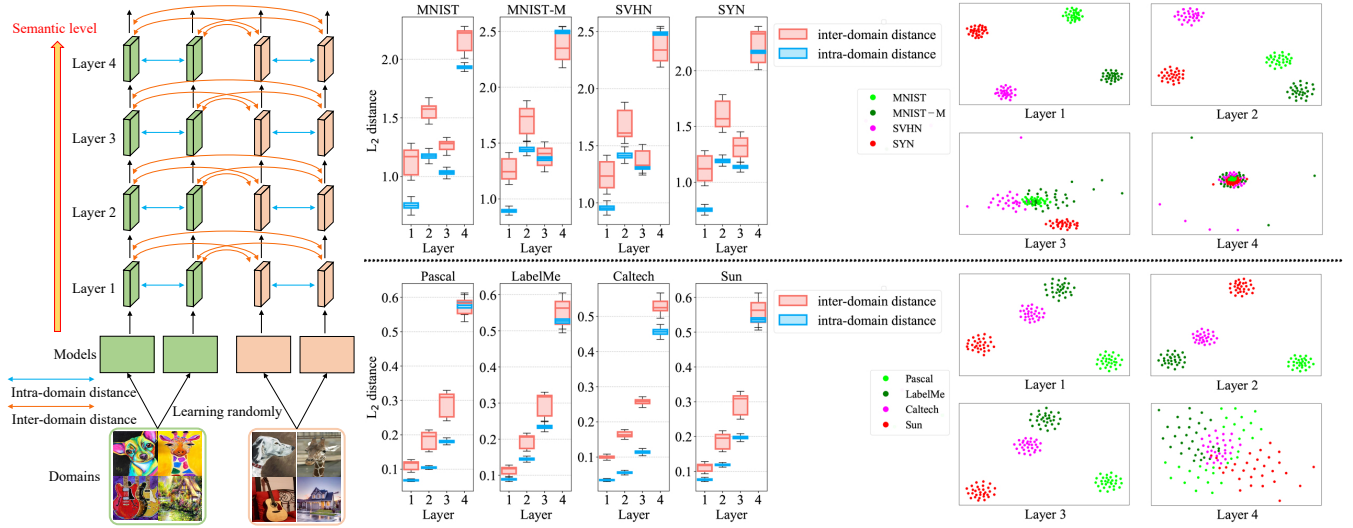


Fig. 4. We randomly run 50 ResNet-18 models on each domain of Digits-DG (top) and VLCS (bottom) datasets, and extract the model parameters of the last convolution layer of the four blocks in ResNet-18 as layer {1, 2, 3, 4}. Left: Diagram of the proof-of-concept experiments; Middle: Average intra-domain and inter-domain L_2 distance of the model parameters in each layer; Right: T-SNE visualization of the model parameter distributions in each layer.

according to their public code, where the boundary component of FedDG is discarded for fair comparison. We use SGD optimizer with learning rate 0.01 and momentum 0.5 for ResNet-18 and MNIST CNN, and learning rate 0.001 for AlexNet. The training epochs for semantic acquisition are set to 30, collaboration rounds for aggregation and calibration are set to 40, for all the datasets. In each round, the calibration epochs are set to 5 and 10 for the Rotated MNIST and the other datasets, respectively. The hyper-parameter λ is set to 0.6 for all the experiments, its sensitivity is further analyzed. We run the experiments on a device with CPU Xeon Gold 6254 \times 2, and GPU Nvidia RTX 2080 TI \times 4. We report the mean and standard error of the classification accuracy over five runs with random seeds for the experiments implemented by us (marked with *). And we cite other results of the DG methods from the published papers like the previous works.

B. Proof-of-Concept Experiments

We randomly run 50 models on each domain of Digits-DG [65] and VLCS datasets, and calculate *intra-domain distance*, i.e., the distance between the models trained on the same domain, and *inter-domain distance* for the models trained on the different domains. The results are shown in Fig. 4, which indicates that: (1) The models trained on the same dataset have closer parameter distributions; (2) The parameter distributions learned from different datasets are closer in higher layers. From observation (1), we find that the model parameters are related to the training data, which verifies our hypothesis. Observation (2) implies that the model parameters in each layer are related to the corresponding semantic level and the information in higher semantic level is more related to the object categories, which is also the latent assumption of domain generalization that one can extract high level discriminative yet domain-agnostic semantics for training a generalizable model.

TABLE I
ACCURACY (%) ON PACS DATASET. “SEP.”: WHETHER USING SEPARATED SOURCE DATASETS. THE BEST RESULTS ARE EMPHASIZED IN BOLD.

Methods	Sep.	Art	Cartoon	Photo	Sketch	Average
DeepAll*	✗	78.95 \pm 0.48	74.90 \pm 1.82	94.08 \pm 0.55	73.02 \pm 0.80	80.24 \pm 0.50
JiGen [4]	✗	79.42	75.25	96.03	71.35	80.51
MASF [9]	✗	80.29	77.17	94.99	71.69	81.04
DGER [64]	✗	80.70	76.40	96.65	71.77	81.38
DMG [6]	✗	76.90	80.38	92.35	75.21	81.46
FACT [55]	✗	85.37	78.38	95.15	79.15	84.51
Epi-FCR [23]	✗	82.1	77.0	93.9	73.0	81.5
MixStyle [67]	✗	84.1	78.8	96.1	75.9	83.7
EISNet [51]	✗	81.89	76.44	95.93	74.33	82.15
FedAvg* [38]	✓	77.49 \pm 0.10	77.21 \pm 0.52	93.56 \pm 0.38	81.19 \pm 0.80	82.36 \pm 0.44
FedDG* [34]	✓	78.46 \pm 0.20	75.98 \pm 0.28	93.23 \pm 0.43	80.92 \pm 0.72	82.15 \pm 0.35
CSAC (ours)	✓	81.98 \pm 0.87	76.41 \pm 0.49	95.20 \pm 0.29	81.64 \pm 0.49	83.81 \pm 0.33

TABLE II
ACCURACY (%) ON VLCS DATASET. “SEP.”: WHETHER USING SEPARATED SOURCE DATASETS. THE BEST RESULTS ARE EMPHASIZED IN BOLD.

Methods	Sep.	Pascal	LabelMe	Caltech	Sun	Average	
						AlexNet	
DeepAll*	✗	71.67 \pm 0.26	59.64 \pm 0.81	97.48 \pm 0.14	67.58 \pm 0.68	74.09 \pm 0.17	
Epi-FCR [23]	✗	67.1	64.3	94.1	65.9	72.9	
JiGen [4]	✗	70.62	60.90	96.93	64.30	73.19	
MASF [9]	✗	69.14	64.90	94.78	67.64	74.11	
DGER [64]	✗	73.24	58.26	96.92	69.10	74.38	
EISNet [51]	✗	69.83	63.49	97.33	68.02	74.67	
FedAvg* [38]	✓	67.92 \pm 0.26	60.23 \pm 0.81	96.85 \pm 0.26	66.88 \pm 0.22	72.97 \pm 0.16	
FedDG* [34]	✓	67.27 \pm 0.07	58.48 \pm 0.04	96.83 \pm 0.47	68.20 \pm 0.12	72.69 \pm 0.16	
CSAC (ours)	✓	70.21 \pm 0.32	58.99 \pm 0.29	97.13 \pm 0.35	67.27 \pm 0.54	73.40 \pm 0.17	
ResNet-18							
DeepAll*	✗	71.40 \pm 0.32	59.77 \pm 0.95	97.54 \pm 0.54	69.01 \pm 0.25	74.43 \pm 0.25	
JiGen* [4]	✗	73.97 \pm 0.21	61.94 \pm 0.74	97.40 \pm 1.03	66.90 \pm 0.64	75.05 \pm 0.26	
FedAvg* [38]	✓	71.95 \pm 0.06	63.29 \pm 0.06	96.48 \pm 0.18	72.37 \pm 0.06	76.02 \pm 0.08	
FedDG* [34]	✓	72.59 \pm 0.30	60.33 \pm 0.07	96.70 \pm 0.20	73.61 \pm 0.17	75.81 \pm 0.16	
CSAC (ours)	✓	71.97 \pm 0.56	63.45 \pm 0.73	97.24 \pm 0.57	72.06 \pm 0.80	76.18 \pm 0.42	

C. Main Results

Table I, II, and III show the results PACS, VLCS, and Rotated MNIST datasets, respectively. We observe that CSAC

TABLE III

ACCURACY (%) ON ROTATED MNIST DATASET. “SEP.”: WHETHER USING SEPARATED SOURCE DATASETS. THE BEST RESULTS ARE EMPHASIZED IN BOLD.

Methods	Sep.	M0	M15	M30	M45	M60	M75	Average
DeepAll*	✗	86.73 \pm 0.45	98.27 \pm 0.40	98.63 \pm 0.15	97.50 \pm 0.89	97.47 \pm 0.25	87.20 \pm 0.95	94.30 \pm 0.29
CrossGrad	✗	86.03	98.92	98.60	98.39	98.68	88.94	94.93
MetaReg [2]	✗	85.70	98.87	98.32	98.58	98.93	89.44	94.97
FeaCri [30]	✗	87.04	99.53	99.41	99.52	99.23	91.52	96.04
DGER [64]	✗	90.09	99.24	99.27	99.31	99.45	90.81	96.36
FedAvg* [38]	✓	82.60 \pm 0.44	98.56 \pm 0.27	98.97 \pm 0.29	93.66 \pm 0.03	95.78 \pm 0.27	86.30 \pm 0.10	92.65 \pm 0.08
FedDG* [34]	✓	73.07 \pm 0.67	94.37 \pm 1.03	95.60 \pm 0.19	89.43 \pm 0.38	94.61 \pm 0.39	84.50 \pm 0.10	88.60 \pm 0.30
CSAC (ours)	✓	84.57 \pm 0.31	98.87 \pm 0.23	98.63 \pm 0.15	95.06 \pm 0.48	96.57 \pm 0.40	90.73 \pm 0.25	94.07 \pm 0.02

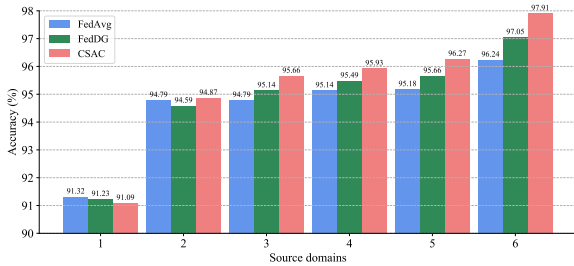


Fig. 5. Results on Office-Caltech-Home dataset. We add one source domain each time from domain set {Am, Cl, Pr, We, Ar, Ca}. Target domain: Rw.

performs the best on about more than half of the separated domain generalization tasks by comparing with FedAvg and FedDG, and also achieves the highest average classification accuracy on all the datasets. We then notice that CSAC can even exhibit comparable or even better model generalization performance than the state-of-the-art DG methods with shared data, especially with larger networks (ResNet-18) and larger datasets (PACS), which indicates that the generalizable model can be effectively trained with separated source domains for privacy protection. Fig. 5 illustrates the results with more source domains, where CSAC shows significant generalization improvement. We attribute it to the effectiveness of collaborative semantic aggregation and calibration of CSAC, and more source domains facilitate the semantic level alignment and domain invariance enhancement during this process.

D. In-Depth Ablation Studies

Semantic aggregation. Table IV reports in-depth ablation results for semantic aggregation. By replacing the strategy with semantic similarity (larger weights for the models that are closer to the average distribution) and average (equal weights), we find that it is important to pay more attention to the domain with the semantic distribution far from the others for fairly absorbing knowledge from all the source domain, facilitating valid domain invariance learning. The experiments with other metrics show the effectiveness of the used L_2 distance.

Semantic calibration. Table V reports in-depth ablation results for semantic calibration. We compare the results without alignment and using the same-layer alignment and find that it is necessary to consider cross-layer semantic relationships for addressing the semantic dislocation problem. By conducting the attention ablations, we demonstrate the attention mechanism with both position and channel interdependency consideration is important for precise semantic

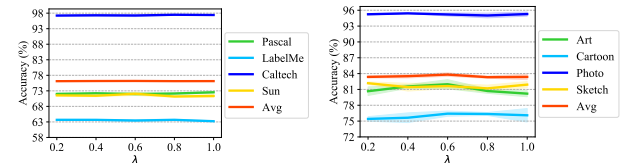


Fig. 6. Sensitivity analysis of the hyper-parameter λ for semantic calibration on VLCS (left) and PACS (right) datasets.

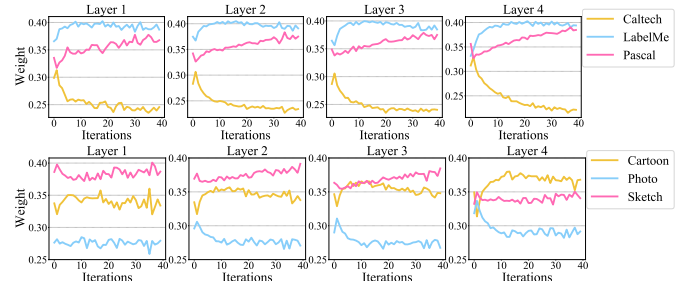


Fig. 7. Semantic divergence based weight for the last layer of the four blocks of ResNet-18 of each trained model (marked with the corresponding domain) during semantic aggregation on VLCS (above) and PACS (below) datasets.

level alignment. The label smoothing is showed useful for a final generalizable model learning, which is may because it leads to more smooth models for stable model fusion. Cross-entropy displays its importance for catastrophic forgetting. The MMD metric is more effective for semantic alignment than the MSE, which may also be the reason that MMD is widely adopted in alignment-based domain adaptation works.

Sensitivity analysis. Fig. 6 shows that CSAC is generally robust to the weight for the semantic calibration, i.e., hyper-parameter λ , which indicate that CSAC might be practical and effective without time-consuming hyper-parameter fine-tuning.

E. Run Time

We report the run time of the methods (implemented locally) in Table VI. FedDG is computationally inefficient by using about three times the run time of FedAvg and CSAC, which is may because of the time-consuming process of the distribution bank building. Besides, FedDG transmits the bank to all the domains, which needs high communication costs and might increase the risks of privacy leakage (although we can not verify it with experiments), as we discussed in related work.

F. Why Does CSAC Work?

In Fig. 7, we observe that the weight curves have the similar trend, i.e., the four extracted layers of each model have the similar semantic divergence to others, which indirectly verifies our hypothesis that parameters are related to the training data. The model with divergent semantics is given large weight layer-by-layer for adequate semantic gathering, facilitating the following semantic calibration, as testified in ablation studies.

Fig. 8 shows comparisons on the learned semantic feature distributions. CSAC obtains more discriminative and domain-agnostic information and generates class clear and domain compact semantic feature representations. We attribute it to

TABLE IV
EFFECT OF SEMANTIC AGGREGATION WITH SEMANTIC DIVERGENCE (STRATEGY) AND L_2 DISTANCE (METRIC).

Type	Case	PACS					VLCS				
		Art	Cartoon	Photo	Sketch	Average	Pascal	LabelMe	Caltech	Sun	Average
Strategy	Semantic similarity	79.22 \pm 0.19	72.44 \pm 0.53	93.00 \pm 0.14	74.34 \pm 0.37	79.75 \pm 0.22	70.80 \pm 0.16	62.86 \pm 0.39	96.61 \pm 0.26	69.49 \pm 1.03	74.94 \pm 0.46
	Semantic average	80.25 \pm 0.36	74.54 \pm 0.44	93.74 \pm 0.15	77.88 \pm 0.69	81.85 \pm 0.07	72.44 \pm 0.17	61.20 \pm 0.32	96.54 \pm 0.30	70.83 \pm 0.45	75.25 \pm 0.21
Metric	Cosine distance	80.89 \pm 0.23	73.57 \pm 0.41	94.43 \pm 0.03	76.59 \pm 1.31	81.37 \pm 0.41	72.27 \pm 0.11	62.94 \pm 0.44	97.05 \pm 0.15	71.41 \pm 0.06	75.92 \pm 0.11
	L_1 distance	81.75 \pm 0.51	74.93 \pm 0.09	94.45 \pm 0.28	77.63 \pm 0.42	82.19 \pm 0.27	72.16 \pm 0.16	64.11 \pm 0.28	96.64 \pm 0.13	71.67 \pm 0.21	76.15 \pm 0.04
CSAC		81.98 \pm 0.87	76.41 \pm 0.49	95.20 \pm 0.29	81.64 \pm 0.49	83.81 \pm 0.33	71.97 \pm 0.56	63.45 \pm 0.73	97.24 \pm 0.57	72.06 \pm 0.80	76.18 \pm 0.42

TABLE V
EFFECT OF SEMANTIC CALIBRATION WITH CROSS-LAYER ALIGNMENT (STRATEGY) AND MMD DISCREPANCY (METRIC).

Type	Case	PACS					VLCS				
		Art	Cartoon	Photo	Sketch	Average	Pascal	LabelMe	Caltech	Sun	Average
Strategy	Without alignment	80.34 \pm 0.24	76.07 \pm 0.14	95.45 \pm 0.49	81.11 \pm 0.12	83.24 \pm 0.15	70.11 \pm 1.21	65.73 \pm 2.31	97.03 \pm 0.15	71.39 \pm 0.16	76.06 \pm 0.75
	Same-layer alignment	80.49 \pm 0.23	74.19 \pm 0.11	94.85 \pm 0.55	80.34 \pm 0.44	82.46 \pm 0.17	73.51 \pm 0.21	62.26 \pm 0.14	97.38 \pm 0.08	71.38 \pm 0.14	76.14 \pm 0.12
	Without attention (position)	79.57 \pm 0.44	73.57 \pm 0.61	94.46 \pm 0.12	79.66 \pm 0.47	81.82 \pm 0.16	72.57 \pm 0.12	63.82 \pm 0.78	96.09 \pm 0.26	69.16 \pm 0.21	75.42 \pm 0.31
	Without attention (channel)	79.80 \pm 0.58	73.77 \pm 0.03	94.43 \pm 0.09	79.32 \pm 0.19	81.83 \pm 0.14	72.40 \pm 0.52	63.54 \pm 0.52	95.92 \pm 0.30	69.24 \pm 0.12	75.27 \pm 0.20
	Without attention	80.35 \pm 0.87	76.27 \pm 0.11	93.59 \pm 0.24	77.88 \pm 1.53	82.02 \pm 0.58	71.63 \pm 0.06	64.48 \pm 2.46	96.27 \pm 0.40	67.67 \pm 1.03	75.01 \pm 0.44
	Without label smoothing	81.78 \pm 1.00	76.37 \pm 0.43	95.00 \pm 0.71	81.46 \pm 0.80	83.65 \pm 0.52	71.70 \pm 0.78	63.33 \pm 0.82	97.17 \pm 0.61	71.34 \pm 1.18	75.89 \pm 0.54
	Without cross-entropy	81.35 \pm 0.09	76.04 \pm 0.17	94.98 \pm 0.39	82.60 \pm 0.50	83.74 \pm 0.13	72.12 \pm 0.23	62.70 \pm 0.16	97.55 \pm 0.21	71.76 \pm 0.23	76.03 \pm 0.10
Metric	Mean Square Error (MSE)	77.08 \pm 0.28	71.05 \pm 1.26	94.61 \pm 0.14	75.99 \pm 0.33	79.68 \pm 0.49	72.10 \pm 0.79	62.17 \pm 0.19	96.47 \pm 0.35	71.09 \pm 0.14	75.46 \pm 0.26
CSAC		81.98 \pm 0.87	76.41 \pm 0.49	95.20 \pm 0.29	81.64 \pm 0.49	83.81 \pm 0.33	71.97 \pm 0.56	63.45 \pm 0.73	97.24 \pm 0.57	72.06 \pm 0.80	76.18 \pm 0.42

TABLE VI
RUN TIME (HOURS) ON PACS AND VLCS DATASETS.

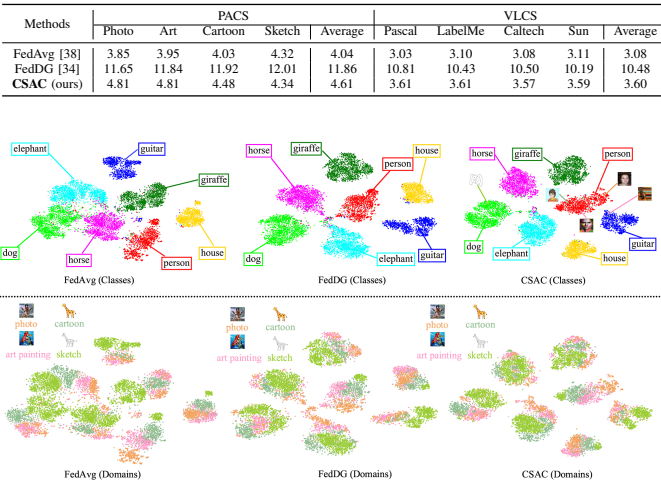


Fig. 8. T-SNE visualization of the learned semantic feature distributions of the data points on PACS dataset (target domain is photo). Different colors represent different classes (above) and domains (below), respectively.

the effectiveness of collaborative semantic aggregation and calibration for domain invariance learning with separated data.

We then present insights on the proposed CSAC via showing the accuracy curves of the models on all the source datasets during training in Fig. 9 (note that the target dataset is only used for testing the model performance). During semantic acquisition, each trained model is assigned to each separated domain for data distribution learning, and its accuracy on the learned domain improves rapidly (see the parts before model fusion in the subfigures (a-c)). The accuracy of the trained models assigned to Art, Cartoon, and Photo domain, on the target dataset, i.e., Sketch (red curve at dotted line), is 52.74%, 68.47%, 32.02%, respectively, before model fusion.

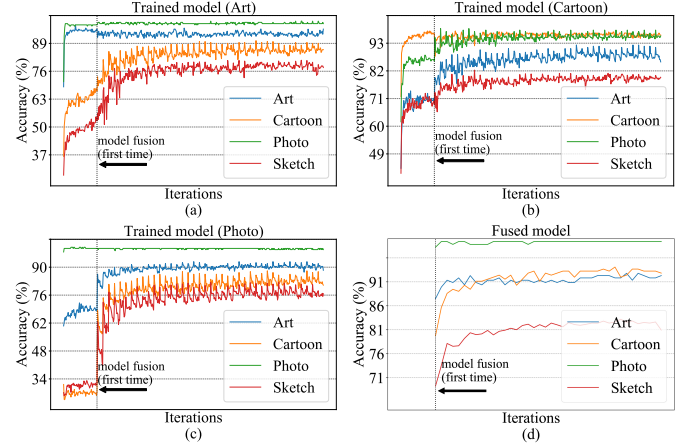


Fig. 9. Accuracy (on all the domains) of the model trained on domain Art (a), Cartoon (b), and Photo (c), and the fused model (d), during the whole training process, i.e., semantic acquisition and the repeat of semantic aggregation and calibration. The adopted dataset (target domain): PACS (Sketch).

Then, the trained models are fused for semantic aggregation, each domain knowledge is fully gathered. The parameters of the fused model are then assigned to each trained model again for semantic calibration with local datasets. We unify semantic learning and alignment by repeating semantic aggregation and calibration alternately, the domain invariance from the separated domains is indirectly captured, making the accuracy of the fused model (subfigure (d)) on all the datasets improve gradually. By comparing the results before model fusion, the accuracy of the trained local model on the target dataset finally reaches improvement of more than 29%, 13%, and 50%.

V. CONCLUSIONS

Training a generalizable model is a vital issue for the deep learning community. However, common practices of domain generalization rely on shared multi-source data, which may

violate privacy policies in many real-world applications. This paper introduces a privacy-preserving task named separated domain generalization, and presents a novel method for this challenging task with collaborative semantic aggregation and calibration. Our method unifies multi-source semantic learning and alignment in a collaborative way, distributed improving model generalization under careful privacy protection. In future, one may be demanded to collaboratively train a generalizable model by exploiting thousands of separated source datasets, which shows the significance of our work in shedding the first light on this promising direction for many privacy-sensitive scenarios like finance and medical care.

ACKNOWLEDGMENTS

This work was supported by Key R & D Projects of the Ministry of Science and Technology (No. 2020YFC0832500), Young Elite Scientists Sponsorship Program by CAST, National Natural Science Foundation of China (No. 62006207), Zhejiang Province Natural Science Foundation (No. LQ21F020020, LZ22F020012).

REFERENCES

- [1] D. Bahdanau, K. Cho, and Y. Bengio. Neural machine translation by jointly learning to align and translate. In *ICLR*, 2015.
- [2] Y. Balaji, S. Sankaranarayanan, and R. Chellappa. Metareg: Towards domain generalization using meta-regularization. In *NeurIPS*, pages 998–1008, 2018.
- [3] G. Blanchard, G. Lee, and C. Scott. Generalizing from several related classification tasks to a new unlabeled sample. *NeurIPS*, 24:2178–2186, 2011.
- [4] F. M. Carlucci, A. D’Innocente, S. Bucci, B. Caputo, and T. Tommasi. Domain generalization by solving jigsaw puzzles. *CVPR*, pages 2224–2233, 2019.
- [5] A. Chadha and Y. Andreopoulos. Improved techniques for adversarial discriminative domain adaptation. *IEEE Transactions on Image Processing (TIP)*, 29:2622–2637, 2019.
- [6] P. Chattopadhyay, Y. Balaji, and J. Hoffman. Learning to balance specificity and invariance for in and out of domain generalization. In *ECCV*, pages 301–318. Springer, 2020.
- [7] Y. Chen, S. Song, S. Li, and C. Wu. A graph embedding framework for maximum mean discrepancy-based domain adaptation algorithms. *IEEE Transactions on Image Processing (TIP)*, 29:199–213, 2019.
- [8] Z. Ding and Y. Fu. Deep domain generalization with structured low-rank constraint. *IEEE Transactions on Image Processing (TIP)*, 27(1):304–313, 2017.
- [9] Q. Dou, D. C. de Castro, K. Kamnitsas, and B. Glocker. Domain generalization via model-agnostic learning of semantic features. In *NeurIPS*, 2019.
- [10] J. Fu, J. Liu, H. Tian, Y. Li, Y. Bao, Z. Fang, and H. Lu. Dual attention network for scene segmentation. In *CVPR*, pages 3146–3154, 2019.
- [11] M. Ghifary, W. Bastiaan Kleijn, M. Zhang, and D. Balduzzi. Domain generalization for object recognition with multi-task autoencoders. In *ICCV*, pages 2551–2559, 2015.
- [12] B. Gholami, P. Sahu, O. Rudovic, K. Bousmalis, and V. Pavlovic. Unsupervised multi-target domain adaptation: An information theoretic approach. *IEEE Transactions on Image Processing (TIP)*, 29:3993–4002, 2020.
- [13] A. Ghosh, J. Chung, D. Yin, and K. Ramchandran. An efficient framework for clustered federated learning. *NeurIPS*, 2020.
- [14] B. Gong, Y. Shi, F. Sha, and K. Grauman. Geodesic flow kernel for unsupervised domain adaptation. In *CVPR*, pages 2066–2073. IEEE, 2012.
- [15] I. J. Goodfellow, M. Mirza, D. Xiao, A. Courville, and Y. Bengio. An empirical investigation of catastrophic forgetting in gradient-based neural networks. *arXiv*, 2013.
- [16] A. Gretton, K. M. Borgwardt, M. J. Rasch, B. Schölkopf, and A. Smola. A kernel two-sample test. *JMLR*, 13(1):723–773, 2012.
- [17] K. He, X. Zhang, S. Ren, and J. Sun. Deep residual learning for image recognition. In *CVPR*, pages 770–778, 2016.
- [18] Z. Huang, H. Wang, E. P. Xing, and D. Huang. Self-challenging improves cross-domain generalization. In *ECCV*, pages 124–140, 2020.
- [19] A. Krizhevsky, I. Sutskever, and G. E. Hinton. Imagenet classification with deep convolutional neural networks. *Commun. ACM*, 60(6):84–90, 2017.
- [20] J. N. Kundu, N. Venkat, R. V. Babu, et al. Universal source-free domain adaptation. In *CVPR*, pages 4544–4553, 2020.
- [21] D. Li, Y. Yang, Y.-Z. Song, and T. Hospedales. Learning to generalize: Meta-learning for domain generalization. In *AAAI*, 2018.
- [22] D. Li, Y. Yang, Y.-Z. Song, and T. M. Hospedales. Deeper, broader and artier domain generalization. In *ICCV*, pages 5542–5550, 2017.
- [23] D. Li, J. Zhang, Y. Yang, C. Liu, Y.-Z. Song, and T. M. Hospedales. Episodic training for domain generalization. *ICCV*, pages 1446–1455, 2019.
- [24] H. Li, S. Jialin Pan, S. Wang, and A. C. Kot. Domain generalization with adversarial feature learning. In *CVPR*, pages 5400–5409, 2018.
- [25] H. Li, Y. Wang, R. Wan, S. Wang, T. Li, and A. C. Kot. Domain generalization for medical imaging classification with linear-dependency regularization. In *NeurIPS*, 2020.
- [26] R. Li, Q. Jiao, W. Cao, H.-S. Wong, and S. Wu. Model adaptation: Unsupervised domain adaptation without source data. In *CVPR*, pages 9641–9650, 2020.
- [27] Y. Li, M. Gong, X. Tian, T. Liu, and D. Tao. Domain generalization via conditional invariant representations. In *AAAI*, 2018.
- [28] Y. Li, W. Hu, H. Li, H. Dong, B. Zhang, and Q. Tian. Aligning discriminative and representative features: An unsupervised domain adaptation method for building damage assessment. *IEEE Transactions on Image Processing (TIP)*, 29:6110–6122, 2020.
- [29] Y. Li, X. Tian, M. Gong, Y. Liu, T. Liu, K. Zhang, and D. Tao. Deep domain generalization via conditional invariant adversarial networks. In *ECCV*, pages 624–639, 2018.
- [30] Y. Li, Y. Yang, W. Zhou, and T. Hospedales. Feature-critic networks for heterogeneous domain generalization. In *ICML*, pages 3915–3924. PMLR, 2019.
- [31] J. Liang, D. Hu, and J. Feng. Do we really need to access the source data? source hypothesis transfer for unsupervised domain adaptation. In *ICML*, pages 6028–6039. PMLR, 2020.
- [32] S. Lin, C.-T. Li, and A. C. Kot. Multi-domain adversarial feature generalization for person re-identification. *IEEE Transactions on Image Processing (TIP)*, 30:1596–1607, 2020.
- [33] T. Lin, L. Kong, S. U. Stich, and M. Jaggi. Ensemble distillation for robust model fusion in federated learning. *NeurIPS*, 2020.
- [34] Q. Liu, C. Chen, J. Qin, Q. Dou, and P.-A. Heng. Feddg: Federated domain generalization on medical image segmentation via episodic learning in continuous frequency space. In *Proceedings of the IEEE/CVF Conference on Computer Vision and Pattern Recognition*, pages 1013–1023, 2021.
- [35] M. Long, H. Zhu, J. Wang, and M. I. Jordan. Unsupervised domain adaptation with residual transfer networks. In *NeurIPS*, 2016.
- [36] T. Matsuura and T. Harada. Domain generalization using a mixture of multiple latent domains. In *AAAI*, 2020.
- [37] M. McCloskey and N. J. Cohen. Catastrophic interference in connectionist networks: The sequential learning problem. In *Psychology of learning and motivation*, volume 24, pages 109–165. Elsevier, 1989.
- [38] B. McMahan, E. Moore, D. Ramage, S. Hampson, and B. A. y Arcas. Communication-efficient learning of deep networks from decentralized data. In *AISTATS*, pages 1273–1282. PMLR, 2017.
- [39] R. Müller, S. Kornblith, and G. E. Hinton. When does label smoothing help? In *NeurIPS*, 2019.
- [40] X. Peng, Z. Huang, Y. Zhu, and K. Saenko. Federated adversarial domain adaptation. *ICLR*, 2020.
- [41] V. Piratla, P. Netrapalli, and S. Sarawagi. Efficient domain generalization via common-specific low-rank decomposition. In *ICML*, 2020.
- [42] F. Qiao, L. Zhao, and X. Peng. Learning to learn single domain generalization. In *CVPR*, pages 12556–12565, 2020.
- [43] J. Quionero-Candela, M. Sugiyama, A. Schwaighofer, and N. D. Lawrence. *Dataset shift in machine learning*. The MIT Press, 2009.
- [44] S. Seo, Y. Suh, D. Kim, J. Han, and B. Han. Learning to optimize domain specific normalization for domain generalization. In *ECCV*, 2020.
- [45] S. Shankar, V. Piratla, S. Chakrabarti, S. Chaudhuri, P. Jyothi, and S. Sarawagi. Generalizing across domains via cross-gradient training. In *ICLR*, 2018.
- [46] H. Venkateswara, J. Eusebio, S. Chakraborty, and S. Panchanathan. Deep hashing network for unsupervised domain adaptation. In *CVPR*, pages 5018–5027, 2017.

- [47] R. Volpi, H. Namkoong, O. Sener, J. C. Duchi, V. Murino, and S. Savarese. Generalizing to unseen domains via adversarial data augmentation. In *NeurIPS*, pages 5334–5344, 2018.
- [48] F. Wang, M. Jiang, C. Qian, S. Yang, C. Li, H. Zhang, X. Wang, and X. Tang. Residual attention network for image classification. In *CVPR*, pages 3156–3164, 2017.
- [49] J. Wang, M.-M. Cheng, and J. Jiang. Domain shift preservation for zero-shot domain adaptation. *IEEE Transactions on Image Processing (TIP)*, 2021.
- [50] Q. Wang, J. Gao, and X. Li. Weakly supervised adversarial domain adaptation for semantic segmentation in urban scenes. *IEEE Transactions on Image Processing (TIP)*, 28(9):4376–4386, 2019.
- [51] S. Wang, L. Yu, C. Li, C.-W. Fu, and P. Heng. Learning from extrinsic and intrinsic supervisions for domain generalization. In *ECCV*, 2020.
- [52] Y. Wang, H. Su, B. Zhang, and X. Hu. Interpret neural networks by identifying critical data routing paths. *CVPR*, pages 8906–8914, 2018.
- [53] Y. Wang, Z. Zhang, W. Hao, and C. Song. Attention guided multiple source and target domain adaptation. *IEEE Transactions on Image Processing (TIP)*, 30:892–906, 2020.
- [54] H. Xu, M. Yang, L. Deng, Y. Qian, and C. Wang. Neutral cross-entropy loss based unsupervised domain adaptation for semantic segmentation. *IEEE Transactions on Image Processing (TIP)*, 30:4516–4525, 2021.
- [55] Q. Xu, R. Zhang, Y. Zhang, Y. Wang, and Q. Tian. A fourier-based framework for domain generalization. In *Proceedings of the IEEE/CVF Conference on Computer Vision and Pattern Recognition*, pages 14383–14392, 2021.
- [56] Q. Yang, Y. Liu, T. Chen, and Y. Tong. Federated machine learning: Concept and applications. *TIST*, 10(2):1–19, 2019.
- [57] T. Yoon, S. Shin, S. J. Hwang, and E. Yang. Fedmix: Approximation of mixup under mean augmented federated learning. In *ICLR*, 2021.
- [58] J. Yuan, X. Ma, D. Chen, K. Kuang, F. Wu, and L. Lin. Collaborative semantic aggregation and calibration for separated domain generalization. *arXiv e-prints*, pages arXiv–2110, 2021.
- [59] J. Yuan, X. Ma, K. Kuang, R. Xiong, M. Gong, and L. Lin. Learning domain-invariant relationship with instrumental variable for domain generalization. *arXiv preprint arXiv:2110.01438*, 2021.
- [60] H. Zhang, I. Goodfellow, D. Metaxas, and A. Odena. Self-attention generative adversarial networks. In *ICML*, pages 7354–7363. PMLR, 2019.
- [61] Q. Zhang, Y. Yang, Y. Wu, and S. Zhu. Interpreting cnns via decision trees. *CVPR*, pages 6254–6263, 2019.
- [62] W. Zhang, D. Xu, J. Zhang, and W. Ouyang. Progressive modality cooperation for multi-modality domain adaptation. *IEEE Transactions on Image Processing (TIP)*, 30:3293–3306, 2021.
- [63] Y. Zhang, Y. Wei, Q. Wu, P. Zhao, S. Niu, J. Huang, and M. Tan. Collaborative unsupervised domain adaptation for medical image diagnosis. *IEEE Transactions on Image Processing (TIP)*, 29:7834–7844, 2020.
- [64] S. Zhao, M. Gong, T. Liu, H. Fu, and D. Tao. Domain generalization via entropy regularization. In *NeurIPS*, 2020.
- [65] K. Zhou, Y. Yang, T. Hospedales, and T. Xiang. Deep domain-adversarial image generation for domain generalisation. In *AAAI*, 2020.
- [66] K. Zhou, Y. Yang, T. Hospedales, and T. Xiang. Learning to generate novel domains for domain generalization. In *ECCV*, pages 561–578, 2020.
- [67] K. Zhou, Y. Yang, Y. Qiao, and T. Xiang. Domain generalization with mixstyle. In *ICLR*, 2021.
- [68] Y. Zuo, H. Yao, and C. Xu. Attention-based multi-source domain adaptation. *IEEE Transactions on Image Processing*, 30:3793–3803, 2021.